SYNTHESIS AND CHARACTERIZATION OF NANO SCALE POROUS SILICON PHOTONIC CRYSTALS FOR OPTICAL DEVICE AND SENSING APPLICATIONS

P. N. PATEL*, V. MISHRA, A. K. PANCHAL[a]
Electronics Engineering Department,
[a]Electrical Engineering Department, S. V. National Institute of Technology, Surat-395007, Gujarat, India

This paper reports the feasibility of synthesis and characterization of One Dimensional nano scale Porous Silicon Photonic Crystals (1D-PSPC) prepared using electrochemical anodization of p-type crystalline silicon wafer by adjusting the current densities. Two structures PSPC1 and PSPC2 with current density 25 and 35mA/cm^2 with 10 minutes of etching time were prepared. Structural and optical properties of the fabricated structures are investigated using Scanning Electron Microscope (SEM), Photoluminescence (PL), reflectance and transmittance. SEM characterization confirms porous structure with average pore size 56.6 nm and 73.9 nm and the thickness 22.5 μm and 23.9 μm for PSPC1 and PSPC2, respectively. PL study shows that the electronic band gap can be tuned from 1.87 eV to 1.93 eV by adjusting the anodization current density at constant electrolyte concentration and etching time. The engineering data reported here are useful for the design and fabrication of the nano scale optical device and sensing applications.

(Received February 13, 2012; Accepted March 5, 2012)

Keywords: Porous Silicon; Photonic Crystals; Electrochemical Anodization; Photoluminescence; Transmittance; Reflectance.

1. Introduction

Photonic crystals are periodic dielectric structures with an index of refraction periodicity of the order of the wavelength of light. They are emerging as a key building block for many applications in nanotechnology that involve controlling the flow of light [1]. In recent years, 1D-PSPC have created great interest of the academic and commercial research in optical devices and sensing. It is emerged as a promising unique material that can provide the link between silicon technology and nano scale optical devices because it is inherently silicon based; therefore the device integration into a standard microelectronics platform is facilitated [2]. PS is a spongy skeleton consist of many pores with silicon network. It is homogeneous mixture of silicon and air. The 1D-PSPC structures are attractive because the properties of a PS layer, such as porosity, thickness, pore size, microstructure are strongly dependent on the anodization conditions [3]. Many research groups all over the world have been working to develop nano optical devices and sensors using PS for the future applications because its optical properties (PL, reflectance) are highly sensitive to the presence of chemical and biological species inside the pores [4]. Several groups have reported the applications of PS nano structures in the optical devices and sensing applications. Fauchet et al. reported work on the optical biosensors applications using nano structure PS [5-6]. C. S. Solanki et al. demonstrated the photovoltaic solar cell applications using PS [7].Sailor research group works on the drug delivery devices and materials using PS [8]. Apart from these, many research groups are working related to characterization and applications for emerging and future nano technology applications using PS [9-16].

*Corresponding author: pnp@eced.svnit.ac.in

In this paper, synthesis and characterization of nano scale 1D-PSPC structures by electrochemical anodization is presented. In section 2, the experimental details for the fabrication of 1D-PSPC structures are presented. In section 3, the structural and optical characterizations of the PS structures is discussed which shows that the average pore size, porosity and film thickness increase with the increase in the current density, while the refractive index and the PL peak decreases, due to the increase in the current density. These results reported will be used for fabrication of multilayer PS based structures such as distributed bragg reflector and microcavity for the organic chemical and bio-sensor applications.

2. Experimental

1D-PSPC structures were fabricated by electrochemical etching of p-type Si wafer (<100>, 0.01- 0.02 ohm-cm, 275 μm, 20 cm^2) by adjusting the anodization current density at constant electrolytes concentration and etching time. The schematic diagram of the electrochemical etching cell is shown in Fig.1.

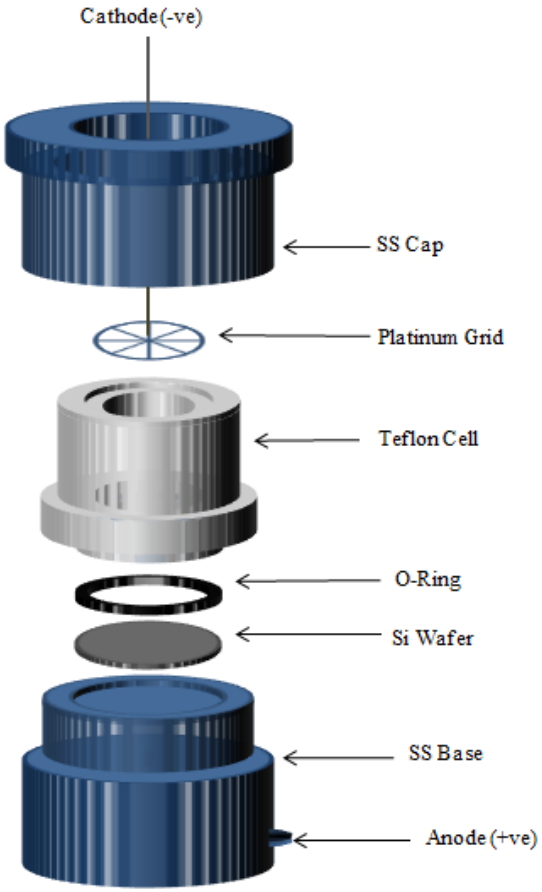

Fig. 1. Electrochemical Etching Cell .

As shown in Fig. 1, the base and the cap of the electrochemical etching cell were made with SS 320 metal. Silicon wafer was placed inside the base and sealed with an O-ring and exposed to the electrolyte. The electrolyte mixture was kept in the highly HF resistant polymer polytetrafluoroethylene (PTFE), which was in contact with the platinum grid, used as a cathode. First, silicon wafer was cleaned using standard piranha cleaning method to remove the organic compounds and other contaminations from the wafer surface and sealed with an O-ring in the cell. PTFE bath was filled with the etching solution of 49% aqueous HF and 99.5% acetic acid, mixed

in the ratio of 1:2. The cathode was immersed in the electrolyte solution and the distance between anode and cathode was kept about 4.5 cm. Periodic constant current square wave was applied by programmable DC power supply (PWS 4305, Tektronix) of the rating 0-5 Amp, 0-30 V DC. A constant current mode was used for anodization process as it was beneficial in terms of regulation [17-18]. Two structures PSPC1 and PSPC2 with current density 25 mA/cm^2 and 35 mA/cm^2 were prepared with constant anodization time of 10 minutes. For transmittance analyses, freestanding films of the same current density were fabricated. Application of high current density (100 mA/cm^2 for 2 minutes) results in the separation of free standing porous silicon film from the Si substrate [18].

After electrochemical etching, these structures were rinsed in DI water for 10 minutes and then dried at room temperature. Structural characterization of the fabricated structures was carried out by SEM (SU1510, Hitachi). The PL was measured by using a monochromator with an attached charge coupled device. A beam of 325 nm line from Helium Cadmium laser at 10 mW output power was used for excitation. The transmittance and reflectance spectra of the structures were measured using spectrometer (MayaPro-2000, Ocean Optics). All measurements were done in the air at room temperature. Polished silicon wafer was used as reference in the reflectance measurements.

3. Results and discussion

Fig. 2 (a) and 2 (b) shows the surface morphology of the structures in SEM plan view for the PSPC1 and PSPC2 structures, respectively. The array of void spaces (dark) in silicon matrix (bright) can be seen clearly in the plan view SEM image. The morphology of the structures shows that the electrochemical etching is done uniformly on the surface and created the granular structure in a spherical shape. Large number of pores distributed in all direction can be observed Fig. 2 (a) and (b).

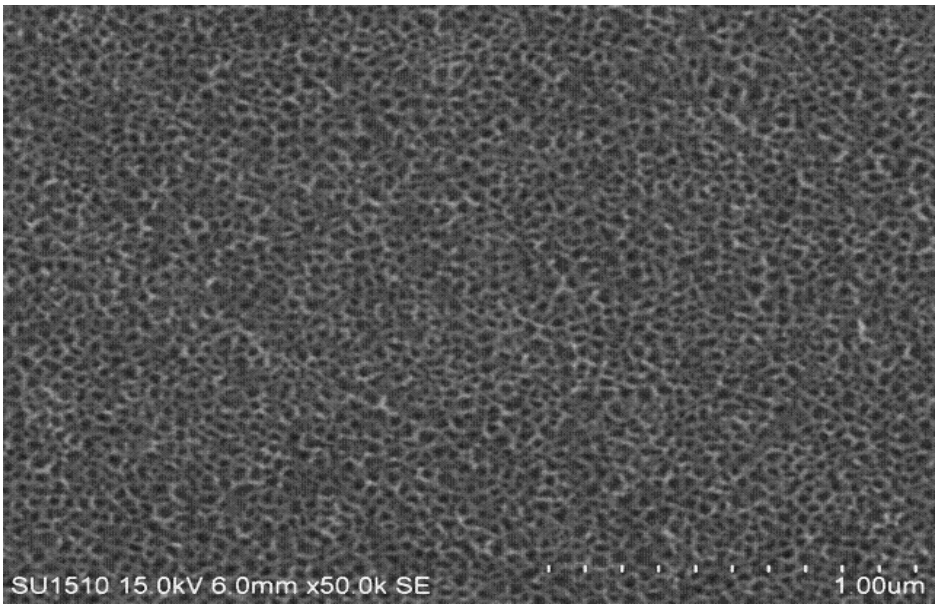

Fig. 2 (a): SEM Plan View of Structure PSPC1

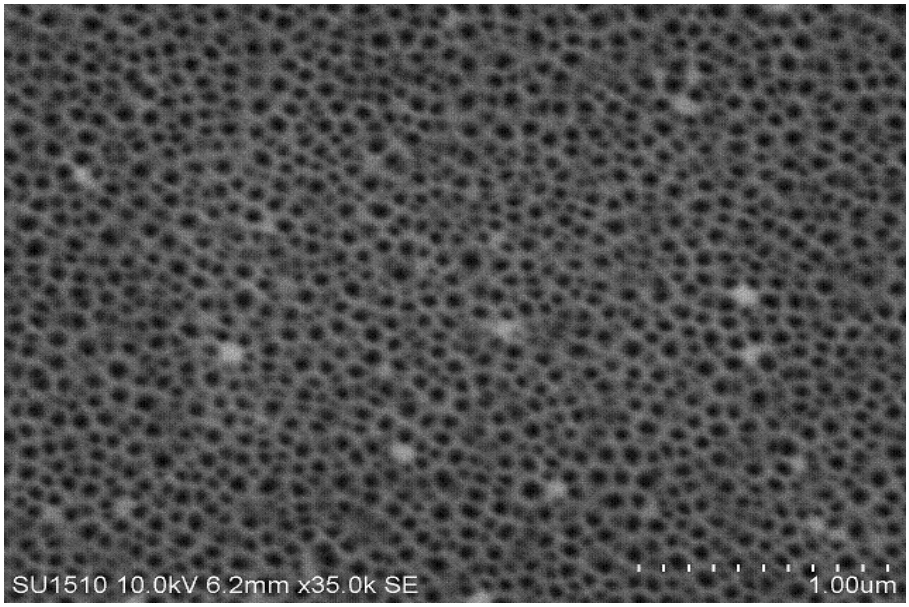

Fig. 2 (b): SEM Plan View of Structure PSPC2.

Pore size analysis of the SEM image is done using particle size analysis software Image J [19]. From this analysis, pore size is observed 56.6 nm and 73.9 nm for PSPC1 and PSPC2 structures, respectively. Due to increase in the current density, silicon network in the porous structure becomes thinner which increases the pore size of the structures [3]. This analysis is helpful in the design of nano scale optical biosensors where pore size is optimized for the specific size of the bio-analyte like bacteria and viruses. Thickness of the PSPC1 and PSPC2 structures are measured by the SEM cross sectional view. SEM cross sectional view of PSPC1 and PSPC2 structures are shown in Fig. 3 (a) and (b), respectively. It is observable that, as the current density increases from J = 25 to 35 mA/cm^2, the thickness of the PSPC1 and PSPC2 structure increases from 22.5 µm to 23.9 µm, due to increase in the current density, more number of holes are available for the etching and pore growth occurs in the depth from the surface to the bottom of the wafer [3-4].

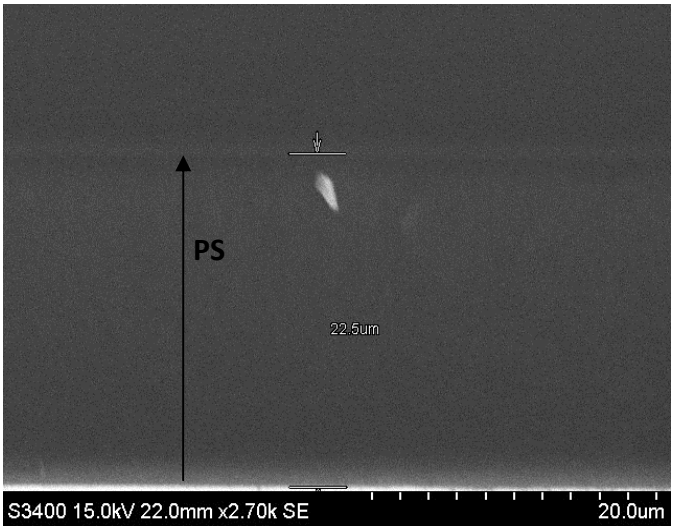

Fig. 3 (a): SEM Cross Section View of PSPC1

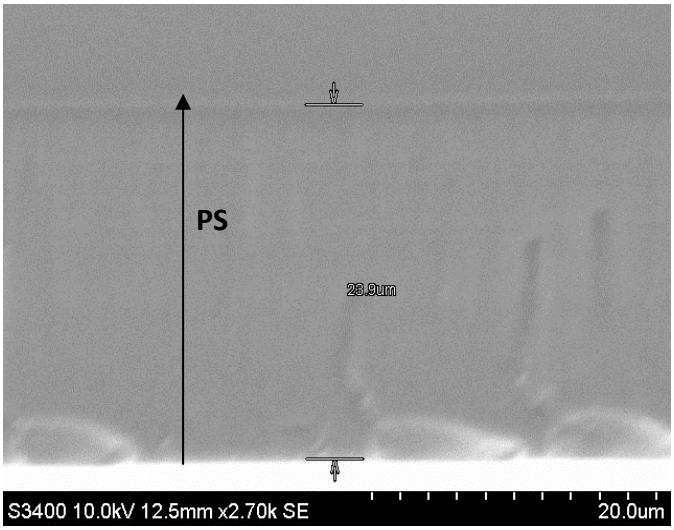

Fig. 3 (b): SEM Cross View of PSPC2

PL is a process in which a substance absorbs photons and then re-radiates photons. This can be described as an excitation to a higher energy state and then a return to a lower energy state accompanied by the emission of a photon. Room temperature PL spectra of structure PSPC1 and PSPC2 are shown in Fig. 4. In PL spectra of Fig. 4, a peak of emission for structure PSPC1 is observed at 660 nm. However, for structure PSPC2 the peak of emission is centred at 640 nm and the band gap is 1.87eV and 1.93 eV for PSPC1 and PSPC2 structures, respectively. The reason for increase in the PL peak can be understood by quantum confinement mechanism [20-21]. According to quantum confinement mechanism, decrease of the mean size of silicon nano particles with increasing current density is revealed in a monotonous blue shift of PL maximum at room temperature of studied structures. Though, correct interpretation of the blue shift of PL spectra requires detailed knowledge of porous silicon morphology. The PL analysis is useful in the design of the nano scale optical bandgap device applications.

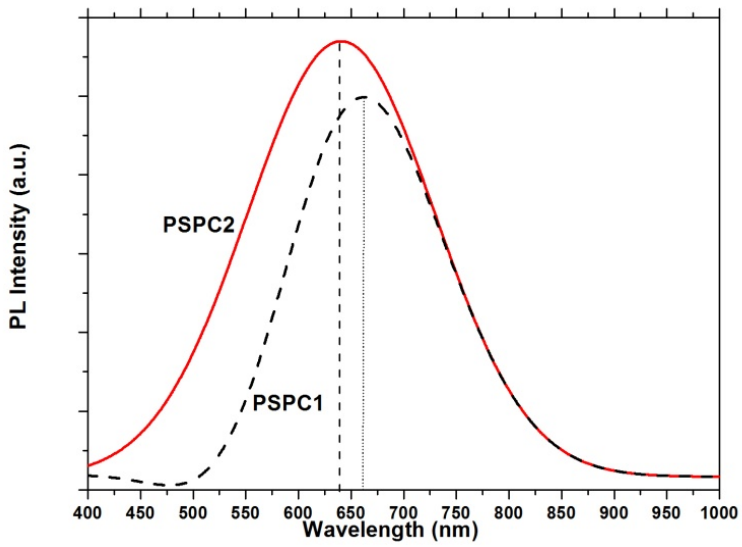

Fig. 4: PL Spectra of PSPC1 and PSPC2

The transmittance of a structure is the ratio of the intensity of the light that has passed through the structure to the intensity of the light when it entered the structure. The transmittance

spectrum of PSPC1 and PSPC2 structures is shown in Fig. 5. It is observed from the transmittance spectra of the prepared structures that free standing porous silicon films have poor transparency at shorter wavelengths (λ<800 nm) [22]. For structures PSPC1 and PSPC2, as current density increases from 25 to 35 mA/cm^2, the transmittance of the structures increases from 33.46% to 42.69%. In this case, due to increase in the current density the mean pore size also increases from 56.6 nm and 73.9 nm. With increase in pore size, passage for light transmission also increases, which increase the transmittance of the structures. The rising transmittance at high current density is indicative of indirect bandgap optical transitions in PSPC structures [3]. The transmittance analysis is useful in the design of the nano scale PS structures for the band pass and stop band optical filters.

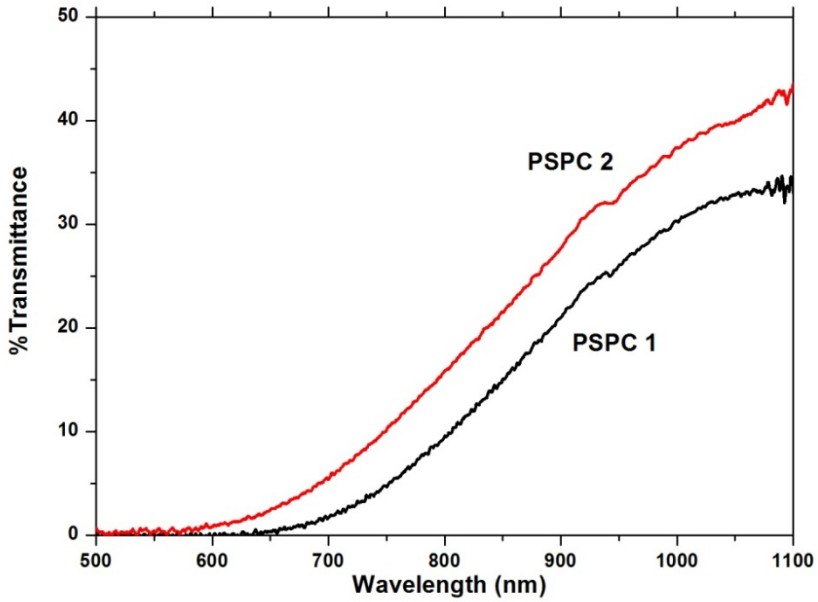

Fig. 5: Wavelength vs. Transmittance

Again, transmittance measurement is important because the absorption coefficient can also measured by optical transmittance measurements [3]. The value of absorption coefficient near band edge provides key information about the film's band structure. The energy gap E_g can be found from the well known relation [12]:

$$\alpha h\nu = A(h\nu - E_g)^m \quad (1)$$

Where,
A is the edge width parameter representing the film quality,
E_g is optical energy gap of material
$m = 1$ for the direct allowed transition and $m = 2$ for the indirect allowed transition.

When, $(\alpha h\nu)^{1/m} = 0$ then $E_g - h\nu$ for certain value of ν. The usual method for the determination of the value of E_g involves a plotting of $(\alpha h\nu)^{1/m}$ *vs* $h\nu$. The value of the energy gap E_g is determined from the intercept of extrapolation to zero absorption with the photon energy axis. Fig. 6 shows the plot of $(\alpha h\nu)^{1/m}$ *vs* $h\nu$, which is used to calculate the energy band gap, considering an indirect allowed transition of PS for structures PSPC1 and PSPC2.

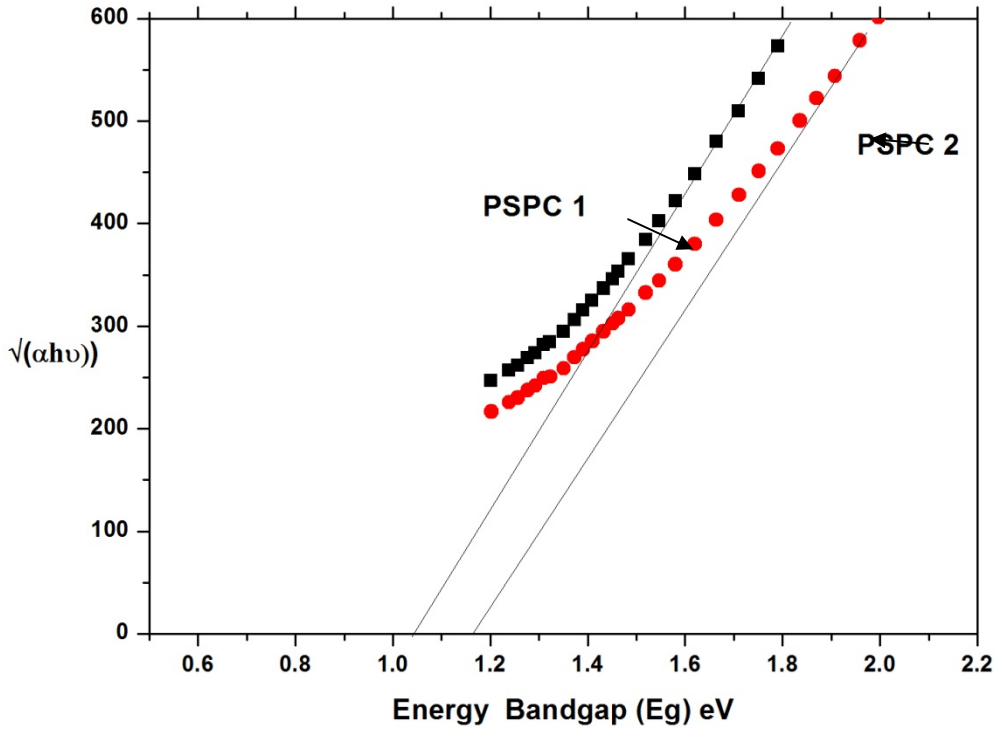

Fig. 6: Wavelength vs Band Gap Energy

It is observed that the indirect energy band gap increases from 1.04 eV to 1.16 eV when current density increases from 25 to 35 mA/cm2 for PSPC1 and PSPC2 structures, respectively Because blue shifts increased with increasing current density or porosity and decreasing average nano crystal size, therefore indicating an opening of the bandgap due to quantum confinement [3-4].

The reflectance spectra of the prepared structures are shown in Fig. 7. The reflectance of PSPC structure strongly depends on the anodization parameters. As the current density is changed, the porosity is also changed for the same structure. Due to which the refractive indices is also changed and as a result of it, the reflectance is varied [23-24]. The refractive indices of the structures are calculated from the measured thickness from the SEM cross section monograms and the Eq. (2) near the 800 nm. Porosity is calculated by the curve fitting method using effective medium theory. It was observed that as the current density increases from 25 to 35 mA/cm^2, the refractive index is reduced from 2.046 to 1.811 while the porosity is increased from 55% to 62% for structures PSPC1 and PSPC2 respectively.

$$n = \frac{1}{2d}\left(\frac{1}{\lambda_r} - \frac{1}{\lambda_{r+1}}\right)^{-1} \qquad (2)$$

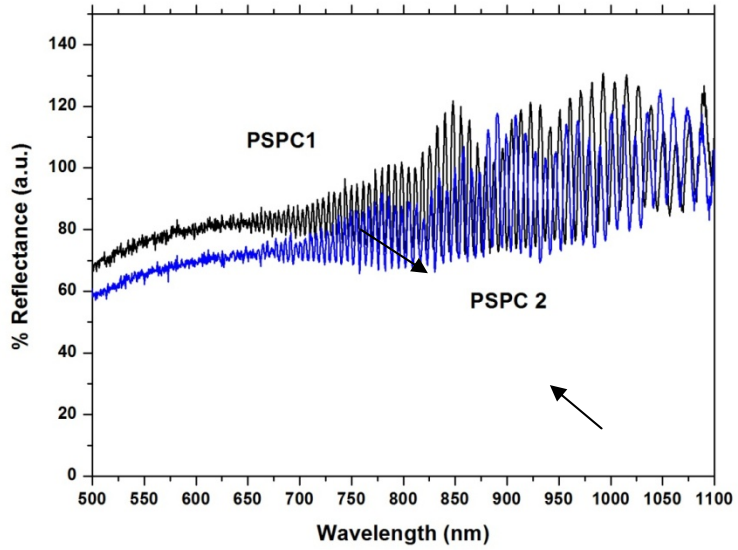

Fig. 7: Wavelength vs. Reflectance plot of PSPC1 and PSPC2

This is expected as the porous silicon is a two phase composite, being a mixture of air and the silicon solid phase. An increase in the current density increases the porosity and hence the amount of air in the pores which decreases the refractive index of the porous silicon. As refractive index decreases, the reflectance also decreases which can be observed in the reflectance spectrum of Fig. 7. Very close fringes are observed in the reflectance spectra (Fig. 7), due to the higher etching time. Also, offset in the reflectance is observed due to the back scattering effect. The reflectance analysis is useful in the design and synthesis of the smart powder for the solar cell applications.

All the engineering data of the physical and optical characterization of the PSPC1 and PSPC2 structures are summarized in the Table 1.

Table 1: Engineering data of the characterization

Structure	Current Density (mA/cm^2)	Surface Characterization			Optical Characterization			
		Pore Size (nm)	Thickness (µm)	Porosity (%)	Refractive Index	PL Peak (nm)	PL Peak (eV)	Transmittance (%)
PSPC1	25	56.6	22.5	55	2.046	660	1.87	33.46
PSPC2	35	73.9	23.9	62	1.811	640	1.93	42.69

The data summarized in Table 1 indicates that; as the current density increases; pore size, physical thickness of the layer, porosity, transmittance, and energy band gap increases while refractive index, reflectance and PL peak decreases. These results are useful for the design of potential applications of nano scale PS based materials for the light emitting devices, photovoltaic solar cells, optical filters, photonic devices like distributed bragg reflectors, microcavity, rugate filters, chemical and bio-sensors.

4. Conclusions

Fabrication and characterization of PS based photonic crystals by electrochemical etching under different current densities were studied. All the properties of 1D-PSPC structures, such as pore size, thickness and porosity are strongly dependent on the anodization conditions. Porous structure is confirmed in the plan view of SEM characterization. Large number of pores uniformly distributed on overall surface with average pore size of 56.6 and 73.9 nm in PSPC1 and PSPC2 respectively, was observed. The photoluminescence emission of 660 nm and 640 nm were observed for the applied current densities due to the quantum confinement effect. The increase in the transmittance and decrease in the reflectance is observed due to the increase in the porosity due to increase in the current density of the structures. It is concluded that quantum confinement plays important role in all the optical characterizations. These results will be used for fabrication of multilayer PS based structures for the organic chemical and bio-sensor applications.

Acknowledgment

This work is supported by the grant from Defence Research and Development Organization (DRDO), Govt. of India.

References

[1] R H Lipson and C Lu, Eur. J. Phys. **30**, S33 (2009).
[2] Thuy Chi Do, Huy Bui, Thuy Van Nguyen, The Anh Nguyen, Thanh Hai Nguyen and Van Hoi Pham, Adv. Nat. Sci.: Nanosci. Nanotechnol. **2**, 35001 (2011).
[3] Liegh Canham (ed.), Properties of Porous Silicon" INSPEC, London, (1997).
[4] A. G. Cullis, L. T. Canham and P. D. J. Calcott, J. Appl. Physics **82**, 3 (1997).
[5] Huimin Ouyang and Philippe M. Fauchet, proceedings of SPIE Optics East, **6005**, 600508 (2005).
[6] N. Koshida (ed.), Device Applications of Silicon Nanocrystals and Nanostructures, Springer Science, (2009).
[7] Kale P. G.; Solanki C. S., 35th IEEE Photovoltaic Specialists Conference (PVSC), 3692 (2010).
[8] Emily J. Anglin, Lingyun Cheng, William R. Freeman, and Michael J. Sailor, Advanced Drug Delivery Reviews, **60**, 1266 (2008).
[9] R. S. Dubey, D. K. Gautam, Chalcogenide Letters **6**, 10, (2009).
[10] M. A. Mahdi, Asmiet Ramizy, Z. Hassan, S. S. Ng, J. J. Hassan, S. J. Kasim, Chalcogenide Letters 9, 1 (2012).
[11] R. S. Dubey, D. K. Gautam, Journal of Optoelectronic and Biomedical Materials **1**, 1 (2009).
[12] A. Mortezaali, S. Ramezani Sani, F. Javani Jooni, Journal of Non-Oxide Glasses, **1**, 3 (2009).
[13] A. Ioanid, M. Dieaconu, S. Antohe, Digest Journal of Nanomaterials and Biostructures, **5**, 4 (2010).
[14] E. Tommasi, Luca De Stefano, Ilaria Rea, Valentina Di Sarno, Lucia Rotiroti, Paolo Arcari, Annalisa Lamberti, Carmen Sanges and Ivo Rendina, "Porous Silicon Based Resonant Mirrors For Biochemical Sensing", Sensors, **8**, pp. 6549-6556, 2008.
[15] H. Saha, International Journal On Smart Sensing And Intelligent Systems, **1**, 1 (2008).
[16] Luca De Stefano, Ivo Rendina, Luigi Moretti, Stefania Tundo, and Andrea Mario Rossi, Applied Optics, **43**, 1 (2004).
[17] C. Solanki, Ph.D. Thesis, Katholieke University Leuven, Belgium (2007).
[18] A. K. Panchal, P.G. Kale and C. S. Solanki, ICAER (2007).
[19] W. S. Rasband, "Image J", National Institute of Health, Bethesda, Maryland, USA, http://rsb.info.nih.gov.ij/.

[20] Daisy Verma, Firoz Khan, S. N. Singh, P. K. Singh, Solar Energy Materials & Solar Cells, **95**,30 (2011).
[21] J. Diana, A. Macek, D. Niznansky, I. Nemec, V. Vrkoslav, T. Chvojka, I. Jelınek, Applied Surface Science, **238**, 169 (2004).
[22] Krisztian Kordas, Andrea Edit Pap, Szabolcs Beke, Seppo Leppavuori, Optical Materials, **25**, 251 (2004).
[23] R. Dubey and D. K. Gautam, Opt Quant Electron, **41**,189 (2009).
[24] Dharmalingam Mangaiyarkarasi, Mark B H Breese, Ow Yueh Sheng, Kambiz Ansari, Chellappan Vijila, and Daniel Blackwood, Proc. of SPIE, 6125, (2006).